Note

New metal complexes of N_2S_2 tetradentate ligands: Synthesis and spectral studies

Mohamad Jaber Al-Jeboori *, Husam H. Al-Tawel, Reyadh Mahmood Ahmad

Department of Chemistry, College of Education, Ibn Al-Haitham, University of Baghdad, P.O. Box 4150, Adamiyah, Baghdad, Iraq

ABSTRACT

New tetradentate ligands 2-(2-mercaptoethylthio)-N-(pyridin-2-ylmethyl)acetamide H_2L^1 and 2-chloro-2-(2-mercaptoethylthio)-N-(pyridin-2-ylmethyl)acetamide H_2L^2 were synthesised from the reaction of 2-aminomethanepyridine with 1,4-dithian-2-one and 3-chloro-1,4-dithian-2-one, respectively. Monomeric complexes of these ligands, of general formulae $K[Cr^{III}(L^n)Cl_2]$, $K_2[Mn^{II}(L^n)Cl_2]$ and $[M(L^n)]$ (M = Fe(II), Co(II), Ni(II), Cu(II), Zn(II), Cd(II) or Hg(II); $n = 1, 2$) are reported. The mode of bonding and overall geometry of the complexes were determined through IR, UV–Vis, NMR and mass spectral studies, magnetic moment measurements, elemental analysis, metal content and conductance. These studies revealed octahedral geometries for the Cr(III), Mn(II) complexes, square planar for Ni(II) and Cu(II) complexes and tetrahedral for the Fe(II), Co(II), Zn(II), Cd(II) and Hg(II) complexes. The study of complex formation *via* molar ratio in DMF solution has been investigated and results were consistent to those found in the solid complexes with a ratio of (M:L) as (1:1).

© 2009 Elsevier B.V. All rights reserved.

1. Introduction

Transition metal complexes containing N, S and/or N, O donors are of special interest due to their applications in biomedical [1,2], biological [3] and asymmetric catalysis [4,5]. Compounds with N and S donor atoms such as N_2S_2 are considered to be good coordinating ligands because they involve both hard nitrogen atoms and soft sulfur atoms. The importance of complexes with N_2S_2 ligands arise from their use in the medical fields for therapeutic and diagnostic purposes [6,7]. One approach in the field of the design of N_2S_2 ligands has to develop metal–sulfur complexes with characteristic redox properties. The intensive study of this field stems from the recognition of redox active nickel, copper, manganese and zinc–sulfur and/or nitrogen cores along with the role of metal oxidoreductases by means of metal complexes with thiolate and amine ligands [8–10]. These complexes become functional models (biomimetics) which are able to react with CO_2, CO or CH_3 moieties. As part of our continuing efforts to synthesise and characterise transition metal chelates using polydentate ligands, we describe here the synthesis and spectral investigation of two new ligands 2-(2-mercaptoethylthio)-N-(pyridin-2-ylmethyl)acetamide H_2L^1 and 2-chloro-2-(2-mercaptoethylthio)-N-(pyridin-2-ylmethyl)acetamide H_2L^2 and some of their metal complexes.

2. Experimental

2.1. Materials and methods

All reagents were commercially available and used without further purification. Solvents were distilled from appropriate drying agents immediately prior to use. 1,4-Dithian-2-one and 3-chloro-1,4-dithian-2-one compounds were prepared by a published method [11].

2.2. Physical measurements

Elemental analyses (C, H and N) were carried out on a Heraeus instrument (Vario EL). IR spectra were recorded as KBr or CsI discs using a Shimadzu FTIR-8300 spectrophotometer from 4000 to 250 cm^{-1}. Electronic spectra were measured from 200 to 900 nm for 10^{-3} M solutions in DMF at 25 °C using a Shimadzu 160 spectrophotometer. Mass spectra were obtained by positive Electron-Impact (EI) and Fast Atom Bombardment (FAB) were recorded on a VG autospec micromass spectrometer. NMR spectra (^1H, ^{13}C, COSY, ^{13}C–^1H correlated NMR) were acquired in DMSO-d_6 solution using Brucker AMX400 MHz and Jeol Lambda 400 MHz spectrometers with tetramethylsilane (TMS) as an internal standard for ^1H NMR analysis. Metals were determined using a Shimadzu (A.A) 680 G atomic absorption spectrophotometer. Chloride was determined using potentiometer titration method on a 686-Titro processor-665Dosimat-Metrohm Swiss. Conductivity measurements

* Corresponding author. Tel.: +964 1 5237396.
E-mail address: mohamadaljeboori@yahoo.com (M.J. Al-Jeboori).

were made with DMF solutions using a Jenway 4071 digital conductivity meter and room temperature magnetic moments were measured with a magnetic susceptibility balance (Jonson Mattey Catalytic System Division).

3. Synthesis

3.1. Preparation of H_2L^1

A mixture of 2-aminomethanepyridine (0.23 g, 2.3 mmol) in dry degassed $CHCl_3$ (10 ml) was added dropwise to a mixture of 1,4-dithian-2-one (0.3 g, 2.3 mmol) in dry degassed $CHCl_3$ (20 ml). The mixture was allowed to stir under nitrogen blanket for 1 h. Solvent was removed under reduced pressure, to give the desired compound as clear yellow oil, yield (0.4 g, 74%). NMR data (ppm), δ_H (400 MHz, DMSO-d_6): 1.3 (1H, t, J_{HH} 8, S–H); 2.9 (4H, m, $C_{1,2}$–H); 3.3 (2H, s, C_3–H), 4.5 (2H, s, C_5–H), 7.3 (2H, m, $C_{7,9}$–H), 7.8 (1H, m, C_8–H), 8.1 (1H, br, N–H), 8.6 (1H, d, J_{HH} 9, C_{10}–H); δ_C (100.63 MHz, DMSO-d_6): 32.5 (C_1), 36.8 (C_2), 37.9 (C_3), 44.5 (C_5), 122.1 (C_9), 122.7 (C_7), 137.7 (C_8), 151.1 (C_{10}), 156.3 (C_6), 169.3 (C=O). The positive (EI) mass spectrum of H_2L^1 showed the parent ion peak at m/z 242 (45%) corresponding to (M^+) and the following fragments; 214 (32%) $(M-CH_2CH_2)^+$, 181.7 (100%) $[M-CH_2CH_2-SH]^+$, 93.4 (66%) $[M-CH_2CH_2SH+SCH_2CONH]^+$.

3.2. Preparation of H_2L^2

H_2L^2 was prepared in the same manner as H_3L^1 but 3-chloro-1,4-dithian-2-one was used in place of 1,4-dithian-2-one. An identical work-up was employed for the product to give H_2L^2 (0.38 g, 77%) as pale yellow oil. NMR data (ppm), δ_H (400 MHz, DMSO-d_6): 2.1 (1H, m, S–H); 2.8–3.5 (6H, m, $C_{1,2,5}$–H); 4.3 (1H, s, C_3–H), 7.4 (2H, m, $C_{7,9}$–H), 7.7 (1H, m, C_8–H), 8.3 (1H, br, N–H), 8.7 (1H, d, C_{10}–H); δ_C (100.63 MHz, DMSO-d_6): 34.3 (C_1), 36.2 (C_2), 45.9 (C_5), 59.8 (C_3), 122.0 (C_9), 123.2 (C_7), 137.0 (C_8), 148.1 (C_{10}), 148.8 (C_6), 158.3 (C=O). The positive FAB mass spectrum of H_2L^2 showed the parent ion peak at m/z 276 (40%) corresponding to $(M)^+$ and the following fragments; 216 (100%) $[M-SCH_2CH_2]^+$, 108 (55%) $[M-SHCH_2CH_2SCCICOH]^+$, 79 (36%) $[M-SHCH_2CH_2SCCICOCH_2NH_2]^+$.

3.3. General synthesis of the complexes with H_2L^1 and H_2L^2 ligands

A solution of the appropriate ligand (1 mmol) and potassium hydroxide (2.2 mmol) in methanol (20 ml) was stirred for 10 min. A methanolic solution (15 ml) of the metal chloride salt (1 mmol) was then added dropwise. The resulting mixture was refluxed under N_2 for 2 h, resulting in the formation of a solid mass which was washed several times with hot methanol. Elemental analysis data, colours and yields for the complexes are given in (Table 1).

Table 1
Colours, yields, elemental analyses, and molar conductance values.

Compound	Colour	Yield (%)	Found (Calc.) (%)					Λ_M (cm^2 Ω^{-1} mol^{-1})
			M	C	H	N	Cl	
H_2L^1	yellow	74		49.3 (49.6)	5.8 (5.7)	11.6 (11.7)		
$K[Cr(L^1)Cl_2]$	green	60	12.5 (12.9)	29.4 (29.8)	3.2 (3.0)	6.8 (7.0)	17.9 (17.6)	74
$K_2[Mn(L^1)Cl_2]$	brown	57	12.1 (12.3)	26.6 (27.0)	2.6 (2.7)	6.4 (6.3)	15.7 (16.0)	143
$[Fe(L^1)]$	red brown	55	19.1 (18.9)	40.4 (40.6)	4.3 (4.1)	9.6 (9.5)		17
$[Co(L^1)]$	brown	88	19.9 (19.7)	39.9 (40.1)	4.1 (4.0)	9.3 (9.4)		23
$[Ni(L^1)]$	dark purple	65	19.5 (19.6)	40.2 (40.1)	3.9 (4.0)	9.5 (9.4)		12
$[Cu(L^1)]$	green	56	20.8 (20.9)	39.2 (39.5)	4.3 (4.0)	9.1 (9.2)		9
$[Zn(L^1)]$	yellow	62	21.5 (21.4)	39.6 (39.3)	3.8 (4.0)	9.4 (9.2)		26
$[Cd(L^1)]$	yellow	63	32.0 (31.9)	33.7 (34.0)	3.1 (3.4)	8.1 (7.9)		14
$[Hg(L^1)]$	grey	62	45.1 (45.5)	27.3 (27.2)	3.0 (2.7)	6.1 (6.4)		19
H_2L^2	yellow	77		43.1 (43.4)	4.5 (4.7)	10.3 (10.1)	12.5 (12.8)	
$K[Cr(L^2)Cl_2]$	green	74	11.8 (11.9)	27.8 (27.5)	2.2 (2.5)	6.3 (6.4)	24.2 (24.4)	87
$K_2[Mn(L^2)Cl_2]$	brown	68	11.4 (11.5)	24.9 (25.1)	2.3 (2.3)	5.5 (5.6)	22.1 (22.2)	159
$[Fe(L^2)]$	brown	75	16.8 (16.9)	36.7 (36.3)	3.7 (3.4)	8.6 (8.5)	10.8 (10.7)	9
$[Co(L^2)]$	brown	66	17.8 (17.7)	35.8 (36.0)	3.5 (3.3)	8.4 (8.4)	10.5 (10.6)	19
$[Ni(L^2)]$	orange brown	83	17.8 (17.6)	36.2 (36.0)	3.5 (3.3)	8.4 (8.4)	10.7 (10.6)	26
$[Cu(L^2)]$	green	68	18.8 (18.8)	35.7 (35.5)	3.5 (3.3)	8.2 (8.3)	10.3 (10.5)	17
$[Zn(L^2)]$	yellow	61	19.3 (19.2)	35.2 (35.3)	3.7 (3.3)	8.2 (8.2)	10.2 (10.4)	27
$[Cd(L^2)]$	yellow	66	28.8 (29.0)	30.7 (31.0)	3.1 (2.9)	7.4 (7.2)	9.3 (9.2)	22
$[Hg(L^2)]$	grey	64	41.8 (42.2)	25.2 (25.3)	2.1 (2.3)	6.0 (5.9)	9.3 (7.5)	13

4. Results and discussion

The new N_2S_2 tetradentate ligands H_2L^1 and H_2L^2 were obtained in good yields by the reaction of 2-aminomethanepyridine with 2-oxo-1,4-dithiacyclohexan H_2L^1 and 3-chloro-2-oxo-1,4-dithiacyclohexane H_2L^2, respectively. The reactions were carried out in $CHCl_3$ under N_2 atmosphere, Scheme 1. In general the ligands contain two labile protons and by removing these protons an anionic-2 tetradentate system is formed. The ligands were characterised by elemental analysis (Table 1), IR (Table 2), UV–Vis (Table 3), mass spectroscopy and ^1H, ^{13}C NMR spectroscopy, respectively. Monomeric complexes of the ligands with Cr^{III}, Mn^{II}, Fe^{II}, Co^{II}, Ni^{II}, Cu^{II}, Zn^{II}, Cd^{II} and Hg^{II} were synthesised by heating 1 mmol of each ligand with 1 mmol of metal chloride, using methanolic potassium hydroxide as a base. The use of a base in these reactions was found to be essential since otherwise only an intractable mixture was recovered. However, in methanolic potassium hydroxide, deprotonation of the ligands occurs facilitating the formation of the complexes $K[Cr^{III}(L^n)Cl_2]$, $K_2[Mn^{II}(L^2)Cl_2]$ and $[M(L^n)]$, where $M =$ Fe(II), Co(II), Ni(II) Cu(II), Zn(II), Cd(II) and Hg(II), $L^n = L^1$ or L^2 (Scheme 2). The complexes are air-stable solids, soluble in DMF and DMSO, sparingly soluble in MeOH, $CHCl_3$, CH_2Cl_2 and not soluble in other common organic solvents. The analytical data (Table 1) agree well with the suggested formulae. The most important infrared bands of the ligands and their complexes together with their assignments are collected in Table 2.

4.1. NMR and IR spectra

The structural information of the ligands can be deduced from NMR spectra. The ^1H and ^{13}C NMR spectra of the ligands displayed signals corresponding to the various proton and carbon nuclei (Section 3). The IR spectra of the free tetradentate ligands show characteristic bands due to the $v(C=O)$, $v(C=N)$, $v(C=C)$ and $v(N-H)$ functional groups. The distinct frequency around 2550–2560 cm^{-1} assigned for $v(S-H)$ band confirms presence of the thiolate group [12]. The IR spectra of the complexes exhibited H_2L^1 and H_2L^2 bands with the appropriate shifts due to complex formation (Table 2). The absence of a peak around 2550 cm^{-1} in all the complexes indicates the deprotonation of (S–H) group upon complex formation. The $v(C=O)$ amide vibration at ca. 1660 cm^{-1} in the free ligands is shifted and observed around 1608–1680 and 1645–1672 cm^{-1} for the H_2L^1 and H_2L^2 complexes, respectively indicating coordination of the nitrogen of the amide group to the metal atoms [13,14]. The $v(C=N)$ stretching of pyridine around 1595 cm^{-1} in the free ligands is shifted to higher frequency and observed around 1605–1635 and 1605–1630 cm^{-1} for the H_2L^1 and H_2L^2 complexes, respectively indicating coordination of nitrogen of the $C=N$ pyridine moiety to the metal atoms [15]. At lower frequency the complexes exhibited bands around 437–550 and 348–390 cm^{-1} which are assigned to the $v(M-N)$ and $v(M-S)$ vibration modes, respectively [16]. The additional bands observed around 283–295 cm^{-1} in $K[Cr^{III}(L^n)Cl_2]$ and $K_2[Mn^{II}(L^n)Cl_2]$ ($n = 1$ or 2) are

assigned to $v(M-Cl)$ vibrations. These vibrations are characteristic of terminally coordinated chloride [17,18].

The ^1H and ^{13}C NMR spectrum of the complex $[Ni(L^1)]$ in DMSO-d_6 showed peaks of coordinated ligand, which are shifted and observed at; δ_H (400 MHz, DMSO-d_6), 4.62 (1 H, d, J_{HH} 12 Hz, C_5–H), 3.85 (1H, d, J_{HH} 15.5 Hz, C_3–H), 3.56 (1 H, d, J_{HH} 12 Hz, C_5–H), 3.27 (1H, d, J_{HH} 15 Hz, C_3–H), 3.22–3.08 (1H, m, C_2–H), 2.11–1.99 (2H, m, C_6–H), 1.98–1.84 (2H, m, C_1–H), 7.60 (1 H, dd, J_{HH} 7.0 and 6.0 Hz, C_9–H), 8.26 (1 H, t, J_{HH} 7.0 Hz, C_8–H), 8.31 (1 H, d, C_7–H), 9.20 (1 H, d, J_{HH} 6.0 Hz, C_{10}–H); δ_C (100.63 MHz, DMSO-d_6), 33.2 (C_1), 40.4 (C_3), 43.7 (C_2), 51.0 (C_5), 124.7 (C_7), 125.3 (C_9), 141.5 (C_8), 154.0 (C_6), 156.1 (C_{10}), 172.5 ($C=O$). The splitting pattern of the complex shows rigidity is generated in the molecule as a result of coordination. In addition, the NMR spectrum confirms the diamagnetism of nickel atom.

4.2. Mass spectra

The mass spectra of the ligands were also consistent with the proposed structural formulae (see Section 3). The positive ion FAB mass spectra for several complexes were reported. The mass spectrum of $[Ni(L^1)]$ showed several peaks corresponding to successive fragmentation of the molecule. The first peak observed at m/z 299 (7%) represents the molecular ion peak of the complex.

Table 2
IR frequencies (cm^{-1}) of the compounds.

Compound	$v(C=O)$	$v(C=N)$	$v(C=C)$	$v(C-S)$	$v(M-N)$	$v(M-S)$	$v(M-Cl)$
H_2L^1	1651	1597	1537	968, 1003			
$K[Cr(L^1)Cl_2]$	1680	1635	1508	1020, 1070	507	385	289
$K_2[Mn(L^1)Cl_2]$	1625	1600	1520	870, 1000	510	380	295
$[Fe(L^1)]$	1608	1615	1500	1081	501	376	
$[Co(L^1)]$	1610	1609	1480	1055	437	385	
$[Ni(L^1)]$	1625	1605	1560	1040	500	366	
$[Cu(L^1)]$	1640	1608	1580	1035	480	392	
$[Zn(L^1)]$	1648	1625	1555	1030	495	354	
$[Cd(L^1)]$	1665	1613	1485	1050, 1110	505	392	
$[Hg(L^1)]$	1660	1615	1560	1020, 1063	515	381	
H_2L^2	1665	1595	1575	1000, 1065			
$K[Cr(L^2)Cl_2]$	1672	1627	1595	1030, 1070	520	370	283
$K_2[Mn(L^2)Cl_2]$	1645	1605	1580	980	490	387	285
$[Fe(L^2)]$	1670	1620	1575	1015	505	373	
$[Co(L^2)]$	1655	1625	1580	1013	502	358	
$[Ni(L^2)]$	1650	1614	1560	1025	500	348	
$[Cu(L^2)]$	1668	1620	1595	1020	455	390	
$[Zn(L^2)]$	1672	1625	1540	1030	550	389	
$[Cd(L^2)]$	1650	1603	1552	1006	495	360	
$[Hg(L^2)]$	1668	1630	1555	1020	504	377	

Scheme 1. Synthesis route of ligands.

$X = H = H_2L^1$; $X = Cl = H_2L^2$

CHCl$_3$, N$_2$, 1 h stirring

Table 3
Magnetic moment and UV–Vis spectral data in DMF solutions.

Compound	μ_{eff} (BM)	Band position (λ nm)	Extinction coefficient ε_{max} (dm^3 mol^{-1} cm^{-1})	Assignments
K[Cr(L^1)Cl$_2$]	3.85	295	390	$\pi \rightarrow \pi^*$
		437	90	$^4A_2g^{(F)} \rightarrow {}^4T_1g^{(F)}$ (ν_2)
		640	70	$^4A_2g^{(F)} \rightarrow {}^4T_2g^{(F)}$ (ν_1) (10 Dq)
K$_2$[Mn(L^1)Cl$_2$]	5.64	256	1700	$\pi \rightarrow \pi^*$
		342	500	CT
		567	70	$^6A_1g^{(S)} \rightarrow {}^4T_1g^{(G)}$
[Fe(L^1)]	5.10	288	400	$\pi \rightarrow \pi^*$
		362	130	CT
		603	110	$^5E_2^{(D)} \rightarrow {}^5T_2^{(D)}$
[Co(L^1)]	3.91	280	390	$\pi \rightarrow \pi^*$
		367	460	CT
		610	92	$^4T_1g(f) \rightarrow {}^4T_1g(p)$
		668	110	$^4T_1g(f) \rightarrow {}^4A_2g(f)$
[Ni(L^1)]	diamagnetic	262	1700	$\pi \rightarrow \pi^*$
		380	1200	CT
		463	230	$^1A_1g \rightarrow {}^1B_1g$
[Cu(L^1)]	1.88	265	1350	$\pi \rightarrow \pi^*$
		339	190	CT
		520	70	$^2B_1g \rightarrow {}^2Eg$
		763	90	$^2B_1g \rightarrow {}^2B_2g$
		810	120	$^2B_1g \rightarrow {}^2A_2g$
[Zn(L^1)]	diamagnetic	273	1400	$\pi \rightarrow \pi^*$
		320	220	CT
[Cd(L^1)]	diamagnetic	268	790	$\pi \rightarrow \pi^*$
		360	250	CT
[Hg(L^1)]	diamagnetic	263	430	$\pi \rightarrow \pi^*$
		338	80	CT
K[Cr(L^2)Cl$_2$]	3.85	391	400	$\pi \rightarrow \pi^*$
		350	610	CT
		318		$^4A_2g^{(F)} \rightarrow {}^4T_1g^{(P)}$ (ν_3) (Calc.)
		600	200	$^4A_2g \rightarrow {}^4T_1g^{(F)}$ (ν_2)
		740	180	$^4A_2g \rightarrow {}^4T_2g^{(F)}$ (ν_1) (10 Dq)
K$_2$[Mn(L^2)Cl$_2$]	5.39	290	350	$\pi \rightarrow \pi^*$
		340	280	CT
		470	80	$^6A_1g \rightarrow {}^4T_2g^{(G)}$
		610	60	$^6A_1g \rightarrow {}^4T_1g^{(G)}$
[Fe(L^2)]	5.78	296	1200	$\pi \rightarrow \pi^*$
		345	380	CT
		750	120	$^5E_2^{(D)} \rightarrow {}^5T_2^{(D)}$
[Co(L^2)]	3.89	298	980	$\pi \rightarrow \pi^*$
		350	430	CT
		642	88	$^4T_1g(f) \rightarrow {}^4T_1g(p)$
		676	94	$^4T_1g(f) \rightarrow {}^4A_2g(f)$
[Ni(L^2)]	diamagnetic	293	910	$\pi \rightarrow \pi^*$
		435	120	$^1A_1g \rightarrow {}^1B_1g$
		550	100	$^1A_1g \rightarrow {}^1B_2g$
[Cu(L^2)]	1.89	296	1700	$\pi \rightarrow \pi^*$
		417	120	$^2B_1g \rightarrow {}^2Eg$
		507	60	$^2B_1g \rightarrow {}^2B_2g$
		890	40	$^2B_1g \rightarrow {}^2A_2g$
[Zn(L^2)]	diamagnetic	286	680	$\pi \rightarrow \pi^*$
		315	770	CT
[Cd(L^2)]	diamagnetic	282	890	$\pi \rightarrow \pi^*$
		301	920	CT
[Hg(L^2)]	diamagnetic	286	1030	$\pi \rightarrow \pi^*$
		366	680	CT

Other distinct peaks were observed in the mass spectrum at m/z 254, 107 and 58 can be assigned to the (CH$_3$NiSH) fragment and the final metal residue (Ni). The spectrum of [Cd(L^1)] showed several peaks in the mass spectrum at m/z 358 and 112 assigned to molecular ion peak of the complex and the metal residue, respectively. These results are similar to those of analogous complexes reported earlier by others [19,20]. The mass spectrum of [Ni(L^2)] showed the following ion peaks at m/z 332 and 199 assigned to

the molecular ion peak and the (SHNiSNCH$_2$CHCl) fragment, respectively.

4.3. Electronic spectra, magnetic moments and conductivity measurements

The UV–Vis spectra of H$_2$L^1 and H$_2$L^2 exhibits an intense absorption peak at 312 and 345 nm assigned to overlap of $\pi \rightarrow \pi^*$ and $n \rightarrow \pi^*$ transitions. The electronic spectra of the complexes of H$_2$L^1 exhibited various extents of hypsochromic shift of the bands related to the intra-ligand $\pi \rightarrow \pi^*$ transition (Table 3). Bands related to the (CT) transition were observed in the spectra of the complexes (Table 3). The electronic spectrum of the Cr(III) complex displayed two additional bands, which could be attributed to the spin allowed d–d transitions $^4A_2g^{(F)} \rightarrow {}^4T_1g^{(F)}$ (ν_2), $^4A_2g^{(F)} \rightarrow {}^4T_2g^{(F)}$ (ν_1) (10 Dq) and spin forbidden transition $^4A_2g \rightarrow {}^2T_1g$, $^2Eg^{(G)}$ (ν_3), respectively [21–23]. The band related to the ν_3 may be located at higher wave number and hidden by the (CT) or ligand band [21]. These data together with the magnetic moment indicate an octahedral geometry around the Cr(III) atom [24]. The spectrum of the Mn(II) complex showed the $\pi \rightarrow \pi^*$, (CT) transitions and d–d band which could be attributed to spin forbidden transition in an octahedral geometry [21,23,25]. The magnetic moment of this complex is typical for a high spin octahedral structure. The electronic spectra of the Fe(II) and Co(II) complexes are consistent with tetrahedral assignment [21,26]. The magnetic moment of these complexes is typical for a tetrahedral structure. The Ni(II) complex is diamagnetic suggesting a square planar geometry [27]. The electronic spectrum of this complex was consistent with this assignment. The magnetic moment value of the green Cu(II) complex, as well as the other analytical data, are in agreement with square planar structures [21,28–30]. The Cu(II) complex gave brown colour in DMF solutions indicating further coordination to solvent molecules. Thus, the spectrum of the Cu(II) complex in DMF exhibited three low intensity bands which are characteristic of distorted octahedral Cu(II) complexes. The spectra of the Zn(II), Cd(II) and Hg(II) complexes exhibited bands assigned to ligand $\pi \rightarrow \pi^*$ and L $\rightarrow$ M charge transfer [21]. These complexes are diamagnetic as expected. The metals normally prefer tetrahedral coordination. The electronic spectra of the complexes of H$_2$L^2 exhibited bands related to the intra-ligand $\pi \rightarrow \pi^*$ and the (CT) transitions (see Table 3). The spectra of the Cr(III) and Mn(II) complexes of H$_2$L^2 showed similar behaviour to those of H$_2$L^1 suggesting octahedral geometries for the complexes. As for [Co(L^1)] and [Fe(L^1)] the spectra of Co(II) and Fe(II) complexes of H$_2$L^2 together with the μ_{eff} values (Table 3) suggests tetrahedral geometries [21–26]. The spectrum of the Ni(II) and Cu(II) complexes displayed bands characteristic of square planar geometries [21,27–30]. The
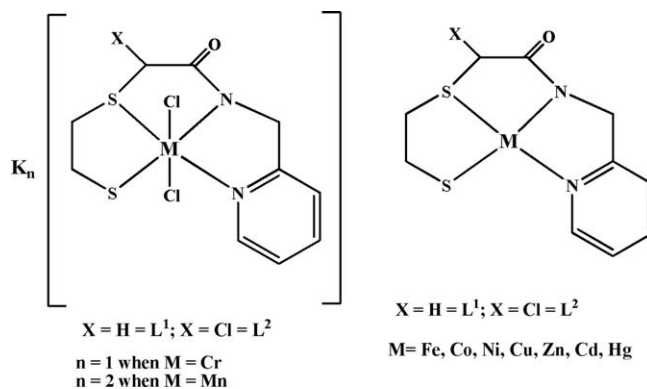
Scheme 2. Proposed structures of metal complexes.

magnetic moment values were consistent with the square planar structures. The spectra of Zn(II), Cd(II) and Hg(II) complexes of H_2L^2 showed similar behaviour to those of H_2L^1 suggesting tetrahedral geometries [21]. The molar conductivities indicate that the Cr(III) complexes are a 1:1 electrolyte, while the Mn(II) complexes are 2:1 and the rest are non-electrolytes (Table 1) [31].

5. Molar ratio

Complex formation by molar ratio of ligand to metal ion was also studied in DMF solution. A series of solutions containing constant concentration of metal ion (1×10^{-3} M) were treated with the same volumes of various concentrations of ligands in presence of potassium hydroxide and heated at 100 °C. The results of L:M titrations were obtained by plotting absorbance of solution mixtures at $\lambda_{\max}$ of the complexes against [L]/[M] which showed a 1:1 M:L ratio for all the complexes, as observed for the solid state.

6. Conclusion

In this paper we have explored the synthesis and coordination chemistry of some monomeric complexes obtained from the reaction of the tetradentate ligands H_2L^1 and H_2L^2 with some metal ions. The mode of bonding and overall structure of the complexes were determined through physico-chemical and spectroscopic methods. Complex formation study *via* molar ratio has been investigated and results were consistent to those found in the solid complexes with a ratio of (M:L) as (1:1).

References

[1] U. Abram, in: J.A. MC Cleverty, T.J. Meyer (Eds.), Comprehensive Coordination Chemistry, second ed., Elsevier, 2004, p. 27.
[2] E. Benoist, J.F. Gestin, Transition Met. Chem. 24 (1999) 42.
[3] A. Nakamura, R. Hahn, K. Tanaka, Y. Nakayama, Inorg. Chem. 6562 (1995) 34.
[4] S. Diltz, G. Aguirre, F. Ortega, P.J. Walsh, Tetrahedron: Asymmetry 8 (1997) 3559.
[5] M.L. Tommasino, M. Casalta, J.A.J. Breuzard, M. Lemaire, Tetrahedron: Asymmetry 11 (2000) 4835.
[6] E.K. John, M.A. Green, J. Med. Chem. 33 (1990) 764.
[7] S. Liu, D.S. Edwards, Chem. Rev. 99 (1999) 2235.
[8] J.R. Dilworth, P. Arnold, D. Morales, Y. Lock wong, Y. Zheng, Mod. Coord. Chem. (2002) 217.
[9] M.V. Rampersad, S.P. Jeffery, J.H. Reibenspies, C.G. Ortiz, D.J. Darensbourg, M.Y. Darensbourg, Angew. Chem., Int. Ed. 44 (2005) 1217.
[10] G. Musie, P.J. Farmer, T. Tuntulani, J.H. Reibenspies, M.Y. Darensbourg, Inorg. Chem. 35 (1996) 2176.
[11] J. Larsen, C. Lenoir, Org. Synth. 72 (1993) 265.
[12] K. Nakamoto, Infrared Spectra of Inorganic and Coordination Compounds, fourth ed., John Wiley and Sons, New York, 1996.
[13] M.J. Al-Jeboori, A.A. Kashta, Mu'tah Lil-Buhuth Wad-Dirasat 18 (3) (2003) 83.
[14] M.J. Al-Jeboori, A.A. Ameer, N.A. Aboud, J Ibn Al-Haitham Pure Appl. Sci. 17 (3) (2004) 80.
[15] A.Z. El-Sonbati, A.A. El-bindary, A.A. Al-Sarawy, Spectrochim. Acta, Part A 58 (2002) 2771.
[16] M.J. Al-Jeboori, A.H. Al-Dujaili, A.E. Al-Janabi, Transition Met. Chem. 34 (2009) 109.
[17] S. Sreedaran, K.S. Bharathi, A.K. Rahiman, L. Jagadish, V. Kaviyarasan, V. Narayanan, Polyhedron 27 (2008) 2931.
[18] V. Ahsen, F. Gök, Ö. Bekaroğlu, J. Chem. Soc., Dalton Trans. (1987) 1827.
[19] F. Mevellec, S. Collet, D. Deniaud, A. Reliquet, J.-C. Meslin, J. Chem. Soc., Perkin Trans. 1 (2001) 3128.
[20] A. Christensen, H.S. Jensen, V. McKee, C.J. McKenzie, M. Munch, Inorg. Chem. 36 (1997) 6080.
[21] A.B.P. Lever, Inorganic Electronic Spectroscopy, second ed., Elsevier Publishing, New York, 1984.
[22] S. Chandra, M. Pundir, Spectrochim. Acta, Part A 69 (2008) 1.
[23] D. Sutton, Electronic Spectra of Transition Metal Complex, first ed., McGraw-Hill Public Co. Ltd., New York, 1969.
[24] N.S. Yousif, K.H. Hegab, A.E. Eid, Syn. React. Inorg. Met. 33 (2003) 647.
[25] A. Shrivastav, N.K. Singh, S.M. Singh, Biometals 16 (2003) 311.
[26] M.M. Aly, A.O. Baghlaf, N.S. Ganji, Polyhedron 4 (1985) 1301.
[27] N. Raman, S. Esthar, C. Thangaraj, J. Chem. Sci. 116 (2004) 209.
[28] A.A. El-Asmy, N.M. El-Metwally, A.A. Abou-Hussen, Int. J. Pure Appl. Chem. 1 (2006) 75.
[29] M.T. Tarafder, K. Chew, K.A. Crouse, M.A. Ali, B.M. Yamin, H.K. Fun, Polyhedron 27 (2002) 2683.
[30] A.O. Baghiaf, M. Ishaq, O.A. Ahmed, M.A. Al-Julani, Polyhedron 4 (1985) 853.
[31] W.J. Geary, Coord. Chem. Rev. 7 (1971) 81.